Chapter 11

References

References

1. Pushpakom, S., et al., *Drug repurposing: progress, challenges and recommendations.* Nature reviews Drug discovery, 2019. 18(1): p. 41-58.
2. Keiser, M.J., et al., *Predicting new molecular targets for known drugs.* Nature, 2009. 462(7270): p. 175-181.
3. Iorio, F., et al., *Identification of small molecules enhancing autophagic function from drug network analysis.* Autophagy, 2010. 6(8): p. 1204-1205.
4. Serra, A., P. Galdi, and R. Tagliaferri, *Machine learning for bioinformatics and neuroimaging.* Wiley Interdisciplinary Reviews: Data Mining and Knowledge Discovery, 2018. 8(5): p. e1248.
5. Smith, S.B., et al., *Identification of common biological pathways and drug targets across multiple respiratory viruses based on human host gene expression analysis.* PloS one, 2012. 7(3): p. e33174.
6. Lengauer, T. and M. Rarey, *Computational methods for biomolecular docking.* Current opinion in structural biology, 1996. 6(3): p. 402-406.
7. Hollingsworth, S.A. and R.O. Dror, *Molecular dynamics simulation for all.* Neuron, 2018. 99(6): p. 1129-1143.
8. Association, A.s., *2019 Alzheimer's disease facts and figures.* Alzheimer's & dementia, 2019. 15(3): p. 321-387.
9. Ferri, C.P., et al., *Global prevalence of dementia: a Delphi consensus study.* The lancet, 2005. 366(9503): p. 2112-2117.
10. Mawuenyega, K.G., et al., *Decreased clearance of CNS β-amyloid in Alzheimer's disease.* Science, 2010. 330(6012): p. 1774-1774.
11. Ghiso, J., et al., *Systemic catabolism of Alzheimer's Aβ40 and Aβ42.* Journal of Biological Chemistry, 2004. 279(44): p. 45897-45908.
12. Mohamed, L.A. and A. Kaddoumi, *In vitro investigation of amyloid-β hepatobiliary disposition in sandwich-cultured primary rat hepatocytes.* Drug Metabolism and Disposition, 2013. 41(10): p. 1787-1796.
13. Yao, Z.X. and V. Papadopoulos, *Function of β-amyloid in cholesterol transport: a lead to neurotoxicity.* The FASEB Journal, 2002. 16(12): p. 1677-1679.
14. Wang, Y., et al., *The combination of ezetimibe and ursodiol promotes fecal sterol excretion and reveals a G5G8-independent pathway for cholesterol elimination [S].* Journal of Lipid Research, 2015. 56(4): p. 810-820.
15. Wang, L.-J. and B.-L. Song, *Niemann–Pick C1-Like 1 and cholesterol uptake.* Biochimica et Biophysica Acta (BBA)-Molecular and Cell Biology of Lipids, 2012. 1821(7): p. 964-972.
16. Kumari, R. and P.L. Joshi, *A review of Japanese encephalitis in Uttar Pradesh, India.* WHO South-East Asia Journal of Public Health, 2012. 1(4): p. 374-395.

17. Lovato, A., C. de Filippis, and G. Marioni, *Upper airway symptoms in coronavirus disease 2019 (COVID-19).* American journal of Otolaryngology, 2020.

18. Printza, A., et al., *Smell and taste loss recovery time in COVID-19 patients and disease severity.* Journal of Clinical Medicine, 2021. 10(5): p. 966.

19. Fotuhi, M., et al., *Neurobiology of COVID-19.* Journal of Alzheimer's disease, 2020. 76(1): p. 3-19.

20. Ashraf, U., et al., *Pathogenicity and virulence of Japanese encephalitis virus: Neuroinflammation and neuronal cell damage.* Virulence, 2021. 12(1): p. 968-980.

21. Ceccarelli, M., et al., *Editorial–Differences and similarities between Severe Acute Respiratory Syndrome (SARS)-CoronaVirus (CoV) and SARS-CoV-2. Would a rose by another name smell as sweet.* European review for medical and pharmacological sciences, 2020. 24(5): p. 2781-2783.

22. Xu, H., et al., *High expression of ACE2 receptor of 2019-nCoV on the epithelial cells of oral mucosa.* International journal of oral science, 2020. 12(1): p. 1-5.

23. Li, Y.C., W.Z. Bai, and T. Hashikawa, *The neuroinvasive potential of SARS-CoV2 may play a role in the respiratory failure of COVID-19 patients.* Journal of medical virology, 2020. 92(6): p. 552-555.

24. Netland, J., et al., *Severe acute respiratory syndrome coronavirus infection causes neuronal death in the absence of encephalitis in mice transgenic for human ACE2.* Journal of virology, 2008. 82(15): p. 7264-7275.

25. McCray Jr, P.B., et al., *Lethal infection of K18-hACE2 mice infected with severe acute respiratory syndrome coronavirus.* Journal of virology, 2007. 81(2): p. 813-821.

26. Filgueira, L. and N. Lannes, *Review of emerging Japanese encephalitis virus: new aspects and concepts about entry into the brain and inter-cellular spreading.* Pathogens, 2019. 8(3): p. 111.

27. Banerjee, A. and A. Tripathi, *Recent advances in understanding Japanese encephalitis.* F1000Research, 2019. 8.

28. Dutta, K. and A. Basu, *Use of minocycline in viral infections.* The Indian journal of medical research, 2011. 133(5): p. 467.

29. Kumar, R., et al., *Role of oral minocycline in acute encephalitis syndrome in India–a randomized controlled trial.* BMC infectious diseases, 2015. 16: p. 1-10.

30. Nikaido, H. and D. Thanassi, *Penetration of lipophilic agents with multiple protonation sites into bacterial cells: tetracyclines and fluoroquinolones as examples.* Antimicrobial agents and chemotherapy, 1993. 37(7): p. 1393-1399.

31. Giuliani, F., W. Hader, and V.W. Yong, *Minocycline attenuates T cell and microglia activity to impair cytokine production in T cell-microglia interaction.* Journal of leukocyte biology, 2005. 78(1): p. 135-143.

32. Popovic, N., et al., *Inhibition of autoimmune encephalomyelitis by a tetracycline.* Annals of Neurology: Official Journal of the American Neurological Association and the Child Neurology Society, 2002. 51(2): p. 215-223.

33. Song, Y., et al., *Minocycline protects PC12 cells from ischemic-like injury and inhibits 5-lipoxygenase activation.* Neuroreport, 2004. 15(14): p. 2181-2184.

34. Sutton, S.S., et al., *Association between the use of antibiotics, antivirals, and hospitalizations among patients with laboratory-confirmed influenza.* Clinical Infectious Diseases, 2021. 72(4): p. 566-573.

35. Pothineni, V.R., et al., *In vitro and in vivo evaluation of cephalosporins for the treatment of Lyme disease.* Drug Design, Development and Therapy, 2018: p. 2915-2921.

36. MI, A.B.W.W.A., K.M.M.S.R. MH, and N.M.A.R. Aslam, *Qamar MU Salamat MKF Baloch Z.* Infect. Drug Resist, 2018. 11: p. 1645-1658.

37. Mendes, R.E., et al., *Update of the telavancin activity in vitro tested against a worldwide collection of Gram-positive clinical isolates (2013), when applying the revised susceptibility testing method.* Diagnostic Microbiology and Infectious Disease, 2015. 81(4): p. 275-279.

38. Vogelgesang, S., et al., *The role of the ATP-binding cassette transporter P-glycoprotein in the transport of β-amyloid across the blood-brain barrier.* Current pharmaceutical design, 2011. 17(26): p. 2778-2786.

39. Colabufo, N.A., et al., *ABC pumps and their role in active drug transport.* Current topics in medicinal chemistry, 2009. 9(2): p. 119-129.

40. Haslam, I.S., et al., *Rifampin and digoxin induction of MDR1 expression and function in human intestinal (T84) epithelial cells.* British journal of pharmacology, 2008. 154(1): p. 246-255.

41. Sun, Y., et al., *Expression of liver X receptor target genes decreases cellular amyloid β peptide secretion.* Journal of Biological Chemistry, 2003. 278(30): p. 27688-27694.

42. Ma, Z., et al., *Liver X receptors and their agonists: targeting for cholesterol homeostasis and cardiovascular diseases.* Current issues in molecular biology, 2017. 22(1): p. 41-64.

43. Kim, J., J.M. Basak, and D.M. Holtzman, *The role of apolipoprotein E in Alzheimer's disease.* Neuron, 2009. 63(3): p. 287-303.

44. Sodhi, R.K. and N. Singh, *Liver X receptors: emerging therapeutic targets for Alzheimer's disease.* Pharmacological Research, 2013. 72: p. 45-51.

45. Nakaya, K., et al., *Cilostazol enhances macrophage reverse cholesterol transport in vitro and in vivo.* Atherosclerosis, 2010. 213(1): p. 135-141.

46. Gonzalez, F.J., *Nuclear receptor controlof enterohepatic circulation.* Comprehensive Physiology, 2012. 2(4): p. 2811.

47. Chothe, P.P. and P.W. Swaan, *Resveratrol promotes degradation of the human bile acid transporter ASBT (SLC10A2).* Biochemical Journal, 2014. 459(2): p. 301-312.

48. Marambaud, P., H. Zhao, and P. Davies, *Resveratrol promotes clearance of Alzheimer's disease amyloid-β peptides.* Journal of Biological Chemistry, 2005. 280(45): p. 37377-37382.

49. Kangueane, P. and C. Nilofer, *Protein-protein docking: methods and tools*, in *Protein-Protein and Domain-Domain Interactions*. 2018, Springer. p. 161-168.

50. Dodacki, A., et al., *Expression and function of Abcg4 in the mouse blood-brain barrier: role in restricting the brain entry of amyloid-β peptide.* Scientific Reports, 2017. 7(1): p. 13393.

51. Morris, G.M., et al., *Automated docking using a Lamarckian genetic algorithm and an empirical binding free energy function.* Journal of computational chemistry, 1998. 19(14): p. 1639-1662.

52. Saraf, P., et al., *Novel 5, 6-diphenyl-1, 2, 4-triazine-3-thiol derivatives as dual COX-2/5-LOX inhibitors devoid of cardiotoxicity.* Bioorganic Chemistry, 2022. 129: p. 106147.

53. Barrett, T., et al., *NCBI GEO: archive for functional genomics data sets—update.* Nucleic acids research, 2012. 41(D1): p. D991-D995.

54. Oshida, K., et al., *Screening a mouse liver gene expression compendium identifies modulators of the aryl hydrocarbon receptor (AhR).* Toxicology, 2015. 336: p. 99-112.

55. Wigger, L., et al., *System analysis of the functional cross-talk between PPARalpha, LXR and FXR in the human HepaRG liver cells.* bioRxiv, 2019: p. 514976.

56. Bindea, G., et al., *ClueGO: a Cytoscape plug-in to decipher functionally grouped gene ontology and pathway annotation networks.* Bioinformatics, 2009. 25(8): p. 1091-1093.

57. Ianevski, A., A.K. Giri, and T. Aittokallio, *SynergyFinder 2.0: visual analytics of multi-drug combination synergies.* Nucleic acids research, 2020. 48(W1): p. W488-W493.

58. Chen, Y., et al., *Antidiabetic drug metformin (GlucophageR) increases biogenesis of Alzheimer's amyloid peptides via up-regulating BACE1 transcription.* Proceedings of the National Academy of Sciences, 2009. 106(10): p. 3907-3912.

59. Park, S.H., et al., *Protective effect of the phosphodiesterase III inhibitor cilostazol on amyloid β-induced cognitive deficits associated with decreased amyloid β accumulation.* Biochemical and biophysical research communications, 2011. 408(4): p. 602-608.

60. Umeda, T., et al., *Rifampicin is a candidate preventive medicine against amyloid-β and tau oligomers.* Brain, 2016. 139(5): p. 1568-1586.

61. Tang, J., K. Wennerberg, and T. Aittokallio, *What is synergy? The Saariselkä agreement revisited.* Frontiers in pharmacology, 2015. 6: p. 181.

62. Yadav, B., et al., *Searching for drug synergy in complex dose–response landscapes using an interaction potency model.* Computational and structural biotechnology journal, 2015. 13: p. 504-513.

63. Zheng, S., et al., *SynergyFinder plus: toward better interpretation and annotation of drug combination screening datasets.* Genomics, Proteomics & Bioinformatics, 2022.

64. Tripathi, M.K., et al., *Computational exploration and experimental validation to identify a dual inhibitor of cholinesterase and amyloid-beta for the treatment of Alzheimer's disease.* Journal of Computer-Aided Molecular Design, 2020. 34(9): p. 983-1002.

65. Iizuka, T., et al., *Preventive effect of rifampicin on Alzheimer disease needs at least 450 mg daily for 1 year: An FDG-PET follow-up study.* Dementia and geriatric cognitive disorders extra, 2017. 7(2): p. 204-214.

66. Turner, R.S., et al., *A randomized, double-blind, placebo-controlled trial of resveratrol for Alzheimer disease.* Neurology, 2015. 85(16): p. 1383-1391.

67. Moussa, C., et al., *Resveratrol regulates neuro-inflammation and induces adaptive immunity in Alzheimer's disease.* Journal of neuroinflammation, 2017. 14(1): p. 1-10.

68. Koenig, A.M., et al., *Effects of the insulin sensitizer metformin in Alzheimer's disease: Pilot data from a randomized placebo-controlled crossover study.* Alzheimer disease and associated disorders, 2017. 31(2): p. 107.

69. Lee, J.-Y., et al., *Efficacy of cilostazol administration in alzheimer's disease patients with white matter lesions: a positron-emission tomography study.* Neurotherapeutics, 2019. 16(2): p. 394-403.

70. Bassendine, M.F., et al., *Is Alzheimer's Disease a Liver Disease of the Brain?* Journal of Alzheimer's Disease, 2020(Preprint): p. 1-14.

71. Wang, J., et al., *A systemic view of Alzheimer disease—insights from amyloid-β metabolism beyond the brain.* Nature reviews neurology, 2017. 13(10): p. 612-623.

72. Sundaram, S., et al., *Mechanism of Dyslipidemia in Obesity—Unique Regulation of Ileal Villus Cell Brush Border Membrane Sodium–Bile Acid Cotransport.* Cells, 2019. 8(10): p. 1197.

73. Mukhopadhyay, S. and D. Banerjee, *A primer on the evolution of aducanumab: the first antibody approved for treatment of Alzheimer's disease.* Journal of Alzheimer's Disease, 2021. 83(4): p. 1537-1552.

74. Ben Aissa, M., et al., *Discovery of nonlipogenic ABCA1 inducing compounds with potential in Alzheimer's disease and type 2 diabetes.* ACS Pharmacology & Translational Science, 2021. 4(1): p. 143-154.

75. Vats, N., et al., *Glibenclamide, ATP and metformin increases the expression of human bile salt export pump ABCB11*. F1000Research, 2020. 9.

76. Benito, E. and A. Barco, *CREB's control of intrinsic and synaptic plasticity: implications for CREB-dependent memory models*. Trends in neurosciences, 2010. 33(5): p. 230-240.

77. Jeon, B.H., et al., *Increased expression of ATP-binding cassette transporter A1 (ABCA1) as a possible mechanism for the protective effect of cilostazol against hepatic steatosis.* Metabolism, 2015. 64(11): p. 1444-1453.

78. LIPAROTI, M., G. MADONNA, and R. MININO, *The role of physical activity and diet in preventing cognitive decline.* Journal of Physical Education & Sport, 2020. 20.

79. Aykac, A. and A.Ö. Sehirli, *The Function and Expression of ATP-Binding Cassette Transporters Proteins in the Alzheimer's Disease.* Global Medical Genetics, 2021. 8(04): p. 149-155.

80. Yulug, B., et al., *Therapeutic role of rifampicin in Alzheimer's disease.* Psychiatry and clinical neurosciences, 2018. 72(3): p. 152-159.

81. Hamilton, M., et al., *The effect of rifampicin, a prototypical CYP3A4 inducer, on erlotinib pharmacokinetics in healthy subjects.* Cancer chemotherapy and pharmacology, 2014. 73(3): p. 613-621.

82. Kaukab, I., et al., *Evaluation of pharmacokinetic interaction of cilostazol with metoclopramide after oral administration in human.* Current Drug Metabolism, 2019. 20(11): p. 924-928.

83. Li, C., et al., *Cholic acid protects in vitro neurovascular units against oxygen and glucose deprivation-induced injury through the BDNF-TrkB signaling pathway.* Oxidative Medicine and Cellular Longevity, 2020.

84. Ackerman, H.D. and G.S. Gerhard, *Bile acids in neurodegenerative disorders.* Frontiers in aging neuroscience, 2016. 8: p. 263.

85. Li, C.-X., et al., *Hyodeoxycholic acid protects the neurovascular unit against oxygen-glucose deprivation and reoxygenation-induced injury in vitro.* Neural regeneration research, 2019. 14(11): p. 1941.

86. Estrada, L.D., et al., *Liver dysfunction as a novel player in Alzheimer's progression: looking outside the brain.* Frontiers in aging neuroscience, 2019. 11: p. 174.

87. Lo, A.C., et al., *Tauroursodeoxycholic acid (TUDCA) supplementation prevents cognitive impairment and amyloid deposition in APP/PS1 mice.* Neurobiology of disease, 2013. 50: p. 21-29.

88. Schmucker, D.L., *Aging and the liver: an update.* The Journals of Gerontology Series A: Biological Sciences and Medical Sciences, 1998. 53(5): p. B315-B321.

89. Morgan, A., et al., *Cholesterol metabolism: A review of how ageing disrupts the biological mechanisms responsible for its regulation.* Ageing research reviews, 2016. 27: p. 108-124.

90. Benedictus, M.R., et al., *Lower cerebral blood flow is associated with faster cognitive decline in Alzheimer's disease.* European radiology, 2017. 27: p. 1169-1175.

91. Wolters, F.J., et al., *Cerebral perfusion and the risk of dementia: a population-based study.* Circulation, 2017. 136(8): p. 719-728.

92. Granger, C.W., *Investigating causal relations by econometric models and cross-spectral methods.* Econometrica: journal of the Econometric Society, 1969: p. 424-438.

93. Granger, C.W., *Testing for causality: a personal viewpoint.* Journal of Economic Dynamics and control, 1980. 2: p. 329-352.

94. Thurman, W.N. and M.E. Fisher, *Chickens, eggs, and causality, or which came first.* American journal of agricultural economics, 1988. 70(2): p. 237-238.

95. Dang, S., et al., *The dynamic programming high-order dynamic Bayesian networks learning for identifying effective connectivity in human brain from fMRI.* Journal of neuroscience methods, 2017. 285: p. 33-44.

96. Detre, J.A. and D.C. Alsop, *Perfusion magnetic resonance imaging with continuous arterial spin labeling: methods and clinical applications in the central nervous system.* European journal of radiology, 1999. 30(2): p. 115-124.

97. Wong, D.F., et al., *In vivo imaging of amyloid deposition in Alzheimer disease using the radioligand 18F-AV-45 (flobetapir F 18).* Journal of nuclear medicine, 2010. 51(6): p. 913-920.

98. Whittington, A. and R.N. Gunn, *Amyloid load: a more sensitive biomarker for amyloid imaging.* Journal of Nuclear Medicine, 2019. 60(4): p. 536-540.

99. St John-Williams, L., et al., *Bile acids targeted metabolomics and medication classification data in the ADNI1 and ADNIGO/2 cohorts.* Scientific data, 2019. 6(1): p. 1-8.

100. LaMontagne, P.J., et al., *OASIS-3: longitudinal neuroimaging, clinical, and cognitive dataset for normal aging and Alzheimer disease.* MedRxiv, 2019: p. 2019.12. 13.19014902.

101. Erlandsson, K., et al., *A review of partial volume correction techniques for emission tomography and their applications in neurology, cardiology and oncology.* Physics in Medicine & Biology, 2012. 57(21): p. R119.

102. Thomas, B.A., et al., *PETPVC: a toolbox for performing partial volume correction techniques in positron emission tomography.* Physics in Medicine & Biology, 2016. 61(22): p. 7975.

103. Luh, W.M., et al., *QUIPSS II with thin-slice TI1 periodic saturation: a method for improving accuracy of quantitative perfusion imaging using pulsed arterial spin labeling.* Magnetic Resonance in Medicine: An Official Journal of the International Society for Magnetic Resonance in Medicine, 1999. 41(6): p. 1246-1254.

104. Mutsaerts, H.J., et al., *ExploreASL: an image processing pipeline for multi-center ASL perfusion MRI studies.* Neuroimage, 2020. 219: p. 117031.

105. Xu, J., et al., *Regional protein expression in human Alzheimer's brain correlates with disease severity.* Communications biology, 2019. 2(1): p. 1-15.

106. Raichle, M.E., *The brain's default mode network.* Annual review of neuroscience, 2015. 38: p. 433-447.

107. Buckner, R.L., et al., *Molecular, structural, and functional characterization of Alzheimer's disease: evidence for a relationship between default activity, amyloid, and memory.* Journal of neuroscience, 2005. 25(34): p. 7709-7717.

108. Wiener, N., et al., *Extrapolation, interpolation, and smoothing of stationary time series: with engineering applications*. Vol. 113. 1949: MIT press Cambridge, MA.

109. Fan, X., Y. Wang, and X.-Q. Tang, *Extracting predictors for lung adenocarcinoma based on Granger causality test and stepwise character selection.* BMC bioinformatics, 2019. 20(7): p. 83-96.

110. Lu, X., L. Su, and H. White, *Granger causality and structural causality in cross-section and panel data.* Econometric Theory, 2017. 33(2): p. 263-291.

111. Reichenheim, M.E. and E.S. Coutinho, *Measures and models for causal inference in cross-sectional studies: arguments for the appropriateness of the prevalence odds ratio and related logistic regression.* BMC medical research methodology, 2010. 10(1): p. 1-12.

112. Wood, A.C., et al., *Inferring causation from cross-sectional data: examination of the causal relationship between hyperactivity–impulsivity and novelty seeking.* Frontiers in genetics, 2011. 2: p. 6.

113. Martín Cervantes, P.A., N. Rueda López, and S. Cruz Rambaud, *A causal analysis of life expectancy at birth. Evidence from Spain.* International journal of environmental research and public health, 2019. 16(13): p. 2367.

114. Yin, J., F. Mutiso, and L. Tian, *Joint hypothesis testing of the area under the receiver operating characteristic curve and the Youden index.* Pharmaceutical statistics, 2021. 20(3): p. 657-674.

115. RoyChoudhury, A., et al., *Analyzing feed-forward loop relationship in aging phenotypes: physical activity and physical performance.* Mechanisms of ageing and development, 2014. 141: p. 5-11.

116. Kim, H.-Y., *Statistical notes for clinical researchers: Sample size calculation 3. Comparison of several means using one-way ANOVA.* Restorative dentistry & endodontics, 2016. 41(3): p. 231-234.

117. Cohen, J., *edition 2. Statistical power analysis for the behavioral sciences. Hillsdale. L*. 1988, Erlbaum Associates.

118. Nunes, A.F., et al., *TUDCA, a bile acid, attenuates amyloid precursor protein processing and amyloid-β deposition in APP/PS1 mice.* Molecular neurobiology, 2012. 45(3): p. 440-454.

119. Ramalho, R.M., et al., *Tauroursodeoxycholic acid suppresses amyloid β-induced synaptic toxicity in vitro and in APP/PS1 mice.* Neurobiology of aging, 2013. 34(2): p. 551-561.

120. Weller, R.O., et al., *Cerebral amyloid angiopathy in the aetiology and immunotherapy of Alzheimer disease.* Alzheimer's research & therapy, 2009. 1(2): p. 1-13.

121. Korte, N., R. Nortley, and D. Attwell, *Cerebral blood flow decrease as an early pathological mechanism in Alzheimer's disease.* Acta Neuropathologica, 2020. 140: p. 793-810.

122. Binnewijzend, M.A., et al., *Cerebral blood flow measured with 3D pseudocontinuous arterial spin-labeling MR imaging in Alzheimer disease and mild cognitive impairment: a marker for disease severity.* Radiology, 2013. 267(1): p. 221-230.

123. Aghakhanyan, G., et al., *The precuneus–a witness for excessive Aβ gathering in Alzheimer's disease pathology.* Neurodegenerative Diseases, 2018. 18(5-6): p. 302-309.

124. MahmoudianDehkordi, S., et al., *Altered bile acid profile associates with cognitive impairment in Alzheimer's disease—an emerging role for gut microbiome.* Alzheimer's & Dementia, 2019. 15(1): p. 76-92.

125. Ricciarelli, R., et al., *Cholesterol and Alzheimer's disease: a still poorly understood correlation.* IUBMB life, 2012. 64(12): p. 931-935.

126. Simons, M., et al., *Cholesterol depletion inhibits the generation of β-amyloid in hippocampal neurons.* Proceedings of the National Academy of Sciences, 1998. 95(11): p. 6460-6464.

127. Hayes, A.W., *Principles and Methods of Toxicology 4Th Ed.* 2001.

128. Pei, S., et al., *Threshold concentration and random collision determine the growth of the huntingtin inclusion from a stable core.* Communications Biology, 2021. 4(1): p. 971.

129. Bangen, K.J., et al., *Cerebral blood flow and amyloid-β interact to affect memory performance in cognitively normal older adults.* Frontiers in aging neuroscience, 2017. 9: p. 181.

130. Payne, T., et al., *Ursodeoxycholic acid as a novel disease-modifying treatment for Parkinson's disease: protocol for a two-centre, randomised, double-blind, placebo-controlled trial, The'UP'study.* BMJ open, 2020. 10(8): p. e038911.

131. Bazzari, F.H., D.M. Abdallah, and H.S. El-Abhar, *Chenodeoxycholic acid ameliorates AlCl3-induced Alzheimer's disease neurotoxicity and cognitive deterioration via enhanced insulin signaling in rats.* Molecules, 2019. 24(10): p. 1992.

132. Elia, A.E., et al., *Tauroursodeoxycholic acid in the treatment of patients with amyotrophic lateral sclerosis.* European journal of neurology, 2016. 23(1): p. 45-52.

133. Obici, L., et al., *Doxycycline plus tauroursodeoxycholic acid for transthyretin amyloidosis: a phase II study.* Amyloid, 2012. 19(sup1): p. 34-36.

134. Min, J.-H., et al., *Oral solubilized ursodeoxycholic acid therapy in amyotrophic lateral sclerosis: a randomized cross-over trial.* Journal of Korean medical science, 2012. 27(2): p. 200-206.

135. Parry, G.J., et al., *Safety, tolerability, and cerebrospinal fluid penetration of ursodeoxycholic acid in patients with amyotrophic lateral sclerosis.* Clinical neuropharmacology, 2010. 33(1): p. 17-21.

136. Reyes, J.F., et al., *Accumulation of alpha-synuclein within the liver, potential role in the clearance of brain pathology associated with Parkinson's disease.* Acta neuropathologica communications, 2021. 9(1): p. 1-20.

137. Vegas-Suárez, S., et al., *Metabolic Diffusion in Neuropathologies: The Relevance of Brain-Liver Axis.* Frontiers in physiology, 2022: p. 929.

138. Sehgal, N., et al., *Withania somnifera reverses Alzheimer's disease pathology by enhancing low-density lipoprotein receptor-related protein in liver.* Proceedings of the National Academy of Sciences, 2012. 109(9): p. 3510-3515.

139. Bhattacharjee, A. and P.K. Roy, *Conjoint hepatobiliary-enterohepatic cycles for amyloid excretion and enhancing its drug-induced clearance: a systems biology approach to Alzheimer's disease.* Journal of Biomolecular Structure and Dynamics, 2022: p. 1-18.

140. Pareek, V., et al., *Patterning of corpus callosum integrity in glioma observed by MRI: Effect of 2D bi-axial lamellar brain architecture.* Journal of Neuro-Oncology, 2019. 144: p. 165-177.

141. Nath, S., et al., *Spreading of neurodegenerative pathology via neuron-to-neuron transmission of β-amyloid.* Journal of Neuroscience, 2012. 32(26): p. 8767-8777.

142. Petersen, R.C., et al., *Alzheimer's disease neuroimaging initiative (ADNI): clinical characterization.* Neurology, 2010. 74(3): p. 201-209.

143. Aisen, P.S., et al., *Clinical Core of the Alzheimer's Disease Neuroimaging Initiative: progress and plans.* Alzheimer's & Dementia, 2010. 6(3): p. 239-246.

144. Bhattacharjee, A., P. Purohit, and P.K. Roy, *Neuroprotective drug discovery from phytochemicals and metabolites for CNS viral infection: A systems biology approach with clinical and imaging validation.* Frontiers in Neuroscience, 2022. 16.

145. Kobro-Flatmoen, A., et al., *Re-emphasizing early Alzheimer's disease pathology starting in select entorhinal neurons, with a special focus on mitophagy.* Ageing Research Reviews, 2021. 67: p. 101307.

146. Aggleton, J.P., et al., *Thalamic pathology and memory loss in early Alzheimer's disease: moving the focus from the medial temporal lobe to Papez circuit.* Brain, 2016. 139(7): p. 1877-1890.

147. Minoshima, S., et al., *Metabolic reduction in the posterior cingulate cortex in very early Alzheimer's disease.* Annals of Neurology: Official Journal of the American Neurological Association and the Child Neurology Society, 1997. 42(1): p. 85-94.

148. Buckner, R.L., J.R. Andrews-Hanna, and D.L. Schacter, *The brain's default network: anatomy, function, and relevance to disease.* Annals of the new York Academy of Sciences, 2008. 1124(1): p. 1-38.

149. Coleman, M.P. and M.R. Freeman, *Wallerian degeneration, wlds, and nmnat.* Annual review of neuroscience, 2010. 33: p. 245-267.

150. White, E.S., F.E. Baralle, and A.F. Muro, *New insights into form and function of fibronectin splice variants.* The Journal of Pathology: A Journal of the Pathological Society of Great Britain and Ireland, 2008. 216(1): p. 1-14.

151. Martin, J.H., *Neuroanatomy text and atlas*. 2012: McGraw-Hill.

152. Lee, P.-L., et al., *Posterior Cingulate Cortex Network Predicts Alzheimer's Disease Progression.* Frontiers in aging neuroscience, 2020. 12: p. 608667.

153. Van Hoesen, G.W., J. Parvizi, and C.-C. Chu, *Orbitofrontal cortex pathology in Alzheimer's disease.* Cerebral Cortex, 2000. 10(3): p. 243-251.

154. Yasmin, H., et al., *Diffusion abnormalities of the uncinate fasciculus in Alzheimer's disease: diffusion tensor tract-specific analysis using a new method to measure the core of the tract.* Neuroradiology, 2008. 50(4): p. 293-299.

155. Costantini, L.C., et al., *Hypometabolism as a therapeutic target in Alzheimer's disease.* BMC neuroscience, 2008. 9(2): p. 1-9.

156. Fudenberg, H.H. and V.K. Singh, *Alzheimer's "syndrome": Prognosis of subsets with different etiology and preliminary effects of immunotherapy.* Drug Development Research, 1988. 15(2-3): p. 165-174.

157. Bassendine, M.F., et al., *Is Alzheimer's disease a liver disease of the brain?* Journal of Alzheimer's Disease, 2020. 75(1): p. 1-14.

158. Malik, M.A., P. Srivastava, and S.B. Ahmad, *Quantitative estimation of phytochemicals and antimicrobial activity of Podophyllum hexandrum.* Int. J. Curr. Sci, 2018. 6: p. 1152-1155.

159. Luo, H.-J., et al., *Docking study on chlorogenic acid as a potential H5N1 influenza A virus neuraminidase inhibitor.* Medicinal Chemistry Research, 2011. 20: p. 554-557.

160. Moon, A., *Therapeutic potential of bioactive phytochemicals by inhibiting β-lactamase of multidrug resistant clinical isolates.* International Journal of Pharmaceutical Sciences and Research (IJPSR), 2015. 6(11): p. 4695-4704.

161. Alberca, R.W., et al., *Perspective: the potential effects of naringenin in COVID-19.* Frontiers in Immunology, 2020. 11: p. 570919.

162. Derosa, G., et al., *Drugs against coronavirus COVID-19 main protease: A drug repurposing approach.* Chemical Phytotherapy & Research, 2020. 35: p. 1230-1236.

163. Kumar, G., et al., *Pharmacokinetics and brain penetration study of chlorogenic acid in rats.* Xenobiotica, 2019. 49(3): p. 339-345.

164. Lawal, M., F.A. Olotu, and M.E. Soliman, *Across the blood-brain barrier: Neurotherapeutic screening and characterization of naringenin as a novel CRMP-2 inhibitor in the treatment of Alzheimer's disease using bioinformatics and computational tools.* Computers in Biology and Medicine, 2018. 98: p. 168-177.

165. Ishisaka, A., et al., *Accumulation of orally administered quercetin in brain tissue and its antioxidative effects in rats.* Free Radical Biology and Medicine, 2011. 51(7): p. 1329-1336.

166. Aronson, A., *Pharmacotherapeutics of the newer tetracyclines.* Journal of the American Veterinary Medical Association, 1980. 176(10 Spec No): p. 1061-1068.

167. Burgos-Ramos, E., L. Puebla-Jiménez, and E. Arilla-Ferreiro, *Minocycline provides protection against β-amyloid (25-35)-induced alterations of the somatostatin signaling pathway in the rat temporal cortex.* Neuroscience, 2008. 154(4): p. 1458-1466.

168. Yeh, F.C., et al., *Mapping immune cell infiltration using restricted diffusion MRI.* Magnetic resonance in medicine, 2017. 77(2): p. 603-612.

169. Yeh, F.-C., V.J. Wedeen, and W.-Y.I. Tseng, *Generalized ${q} $-sampling imaging.* IEEE transactions on medical imaging, 2010. 29(9): p. 1626-1635.

170. Yeh, F.-C., et al., *Deterministic diffusion fiber tracking improved by quantitative anisotropy.* PloS one, 2013. 8(11): p. e80713.

171. Edlow, B.L., et al., *Neuroanatomic connectivity of the human ascending arousal system critical to consciousness and its disorders.* Journal of Neuropathology & Experimental Neurology, 2012. 71(6): p. 531-546.

172. Goodsell, D.S., G.M. Morris, and A.J. Olson, *Automated docking of flexible ligands: applications of AutoDock.* Journal of molecular recognition, 1996. 9(1): p. 1-5.

173. Brown, G.R., et al., *Gene: a gene-centered information resource at NCBI.* Nucleic acids research, 2015. 43(D1): p. D36-D42.

174. Smoot, M.E., et al., *Cytoscape 2.8: new features for data integration and network visualization.* Bioinformatics, 2011. 27(3): p. 431-432.

175. Tang, Y., et al., *CytoNCA: a cytoscape plugin for centrality analysis and evaluation of protein interaction networks.* Biosystems, 2015. 127: p. 67-72.

176. Thomas, P.D., *The gene ontology and the meaning of biological function.* The gene ontology handbook, 2017: p. 15-24.

177. Mi, H., et al., *PANTHER version 11: expanded annotation data from Gene Ontology and Reactome pathways, and data analysis tool enhancements.* Nucleic acids research, 2017. 45(D1): p. D183-D189.

178. Gavras, H. and I. Gavras, *Angiotensin converting enzyme inhibitors. Properties and side effects.* Hypertension, 1988. 11(3_pt_2): p. II37.

179. Vaduganathan, M., et al., *Renin–angiotensin–aldosterone system inhibitors in patients with Covid-19.* New England Journal of Medicine, 2020. 382(17): p. 1653-1659.

180. Towler, P., et al., *ACE2 X-ray structures reveal a large hinge-bending motion important for inhibitor binding and catalysis.* Journal of Biological Chemistry, 2004. 279(17): p. 17996-18007.

181. Yan, R., et al., *Structural basis for the recognition of SARS-CoV-2 by full-length human ACE2.* Science, 2020. 367(6485): p. 1444-1448.

182. Lan, J., et al., *Structure of the SARS-CoV-2 spike receptor-binding domain bound to the ACE2 receptor.* nature, 2020. 581(7807): p. 215-220.

183. Jin, Z., et al., *Structure of Mpro from SARS-CoV-2 and discovery of its inhibitors.* Nature, 2020. 582(7811): p. 289-293.

184. Nath, M. and B. Deb, *A computational approach of antibiotics as novel drug target for Japanese encephalitis virus NS helicase/nucleoside triphosphatase.* MOJ Proteomics Bioinf, 2018. 7: p. 184-189.

185. Paterson, R.W., et al., *The emerging spectrum of COVID-19 neurology: clinical, radiological and laboratory findings.* Brain, 2020. 143(10): p. 3104-3120.

186. Meinhardt, J., et al., *Olfactory transmucosal SARS-CoV-2 invasion as a port of central nervous system entry in individuals with COVID-19.* Nature neuroscience, 2021. 24(2): p. 168-175.

187. Zink, M.C., et al., *Neuroprotective and anti–human immunodeficiency virus activity of minocycline.* Jama, 2005. 293(16): p. 2003-2011.

188. Michaelis, M., et al., *Minocycline inhibits West Nile virus replication and apoptosis in human neuronal cells.* Journal of antimicrobial chemotherapy, 2007. 60(5): p. 981-986.

189. Mishra, M.K. and A. Basu, *Minocycline neuroprotects, reduces microglial activation, inhibits caspase 3 induction, and viral replication following Japanese encephalitis.* Journal of neurochemistry, 2008. 105(5): p. 1582-1595.

190. Zhao, J., et al., *Recent advances on viral manipulation of NF-κB signaling pathway.* Current opinion in virology, 2015. 15: p. 103-111.

191. Alam, M.A., V. Subramanyam Rallabandi, and P.K. Roy, *Systems biology of immunomodulation for post-stroke neuroplasticity: multimodal implications of pharmacotherapy and neurorehabilitation.* Frontiers in neurology, 2016. 7: p. 94.

192. Amruta, N., et al., *SARS-CoV-2 mediated neuroinflammation and the impact of COVID-19 in neurological disorders.* Cytokine & growth factor reviews, 2021. 58: p. 1-15.

193. Zakeri, B. and G.D. Wright, *Chemical biology of tetracycline antibiotics.* Biochemistry and Cell Biology, 2008. 86(2): p. 124-136.

194. Humar, A., et al., *Severe acute respiratory syndrome and the liver.* Hepatology (Baltimore, Md.), 2004. 39(2): p. 291.

195. Phillips, J.M., T. Gallagher, and S.R. Weiss, *Neurovirulent murine coronavirus JHM. SD uses cellular zinc metalloproteases for virus entry and cell-cell fusion.* Journal of virology, 2017. 91(8): p. e01564-16.

196. Ding, Y., et al., *Antiviral activity of chlorogenic acid against influenza A (H1N1/H3N2) virus and its inhibition of neuraminidase.* Scientific reports, 2017. 7(1): p. 45723.

197. Wang, W.-X., et al., *Chlorogenic acid, a natural product as potential inhibitor of COVID-19: virtual screening experiment based on network pharmacology and molecular docking.* Natural Product Research, 2022. 36(10): p. 2580-2584.

198. Derosa, G., et al., *A role for quercetin in coronavirus disease 2019 (COVID-19).* Phytotherapy Research, 2021. 35(3): p. 1230-1236.

199. Shah, Z., et al., *Podophyllotoxin: history, recent advances and future prospects.* Biomolecules, 2021. 11(4): p. 603.

200. Shah, V.K., et al., *Overview of immune response during SARS-CoV-2 infection: lessons from the past.* Frontiers in immunology, 2020. 11: p. 1949.

201. Nandi, A., et al., *Global and regional projections of the economic burden of Alzheimer's disease and related dementias from 2019 to 2050: A value of statistical life approach.* EClinicalMedicine, 2022. 51: p. 101580.

APPENDIX

1.2.2 Alzheimer's disease pathophysiology

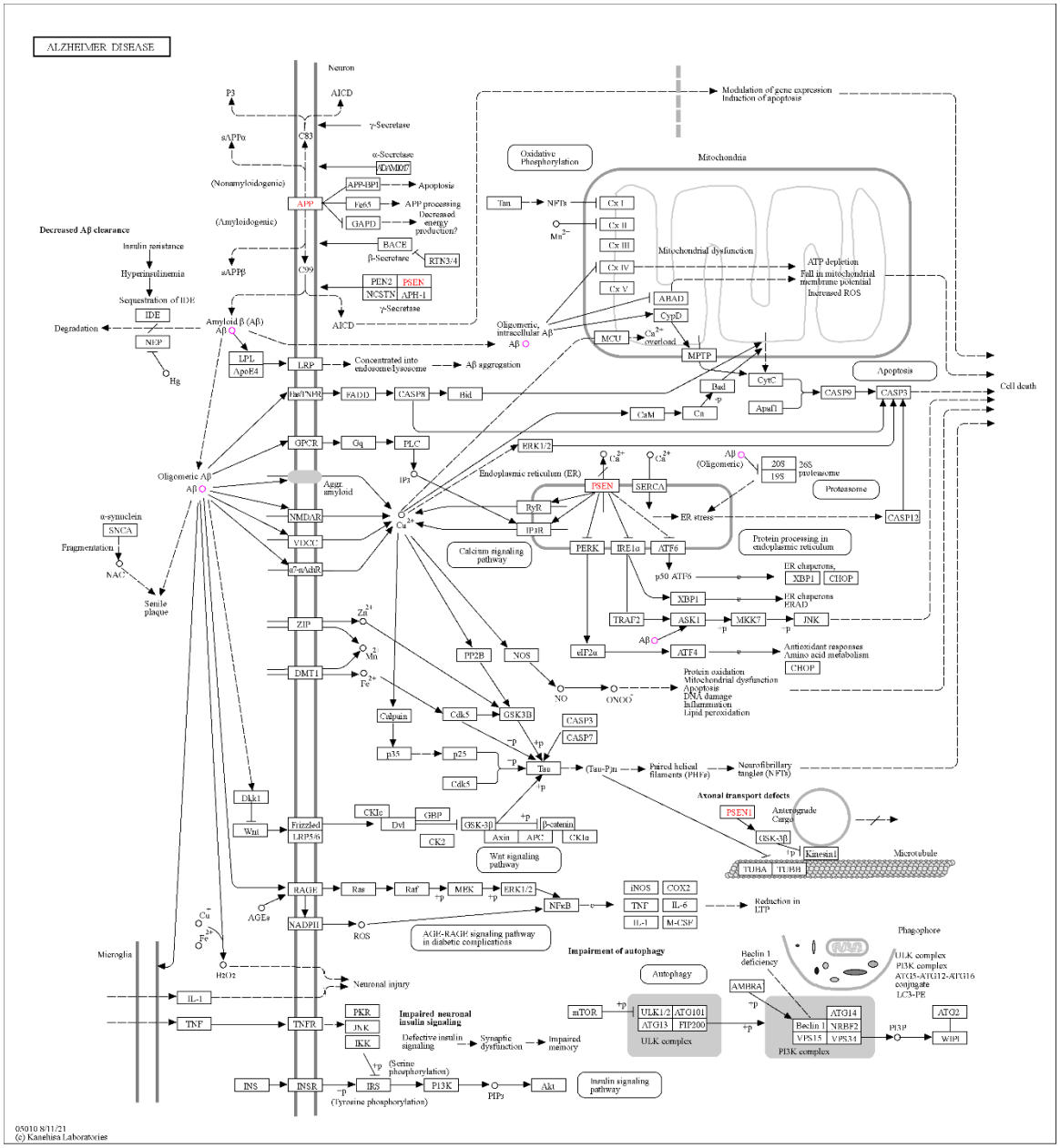

Figure S1: The KEGG pathway of Alzheimer's Disease (map05010).

5.2.5 Amyloid Load: Florbetapir PET Data Acquisition and Processing

Steps for calculating regional values of the Standard Uptake Value Ratio (SUVR) from the Positron Emission Tomography (PET) scans

GitHub repository (https://github.com/pratik-purohit/PET_SUVR)

Step-1

T1-PET co-registration:

Step-2

Bring T1 image in MNI space:

FLIRT (incorrectly oriented & cost-function: Mutual information)

Step-3

Mask formation: Same for other ROIs

fslmaths mni_prob_Cerebellum.nii.gz -thr 10 mask

fslmaths mask.nii.gz –bin mask_bin.nii.gz

use same for pons and add the masks

Step-4

Bring masks to sub-space:

convert_xfm -omat MNI-to-sub.mat -inverse t1_MNI.mat

flirt -in mask_bin_cerebellum_pons.nii.gz -ref t1.nii -out

mask_cerebellum_pons_sub_space -init MNI-to-sub.mat -applyxfm

fslmaths mask_cerebellum_pons_sub_space –bin

mask_cerebellum_pons_sub_space_binary

Step-5

Intensity normalization using pons and cerebellum:

fslmaths co-registered-sub-ADNI011S4827_ses-M05_task-rest_acq-AV45_pet.nii.gz -mul mask_cerebellum_pons_sub_space.nii.gz only-cer-pet.nii.gz

fslstats only-cer-pet.nii.gz -M

fslmaths co-registered-sub-ADNI011S4827_ses-M05_task-rest_acq-AV45_pet.nii.gz -div 2658.717876 normalized_pet_image.nii.gz

Step-6

Apply PET-PVC:

pvc_make4d -i talairach_label_all.nii.gz -o talairach-4DMASK.nii.gz

Bring normalized image in MNI space and apply PET-PVC

petpvc -i normalized_MNI_pet_image.nii.gz -m talairach-4DMASK.nii.gz -o normalized_talairach_pet_pvc_image.nii.gz --pvc IY -x 7.67 -y 7.67 -z 7.5

Bring PET-PVC image in subject space

flirt -in normalized_talairach_pet_pvc_image.nii.gz -ref t1.nii -out normalized_talairach_pet_pvc_sub_space.nii.gz -init MNI-to-sub.mat -applyxfm

Step-7

Multiply with mask to obtain required region wise SUVR in subject space

fslmaths normalized_talairach_pet_pvc_sub_space.nii.gz –mul

mask_precuneus_sub_space.nii.gz only-precuneous-pet-pvc-talairach_sub_space.nii.gz

fslstats only-precuneous-pet-pvc-talairach_sub_space.nii.gz -M

5.2.6 Cerebral Blood Flow - MRI Arterial Spin Tagging analysis

Steps for calculating cerebral blood flow from the Arterial Spin Labelling (ASL) scans

Step 1

Download ExploreASl and Customscript codes for ADNI to BIDS data conversion

GitHub - ExploreASL/CustomScripts: scripts & code snippets used in multiple ASL studies, alongside ExploreASL

Step 2

Extract the files from the ADNI folder of Customscript in the ExploreASL main directory

Step 3

1. Create two folders test_in, test_out and one data.tsv file in a master folder
2. Copy downloaded ADNI data and paste it into the test_in folder

Step 4

Create an userConfig.json file and paste it into ExploreASL main directory

Below information needs to be written in the userConfig.json file, which is basically the paths to the above-mentioned folders.

```
{
   "ADNI_ORIGINAL_DIR": "/path_to_your_drive/test_in",
   "ADNI_OUTPUT_DIR": "/path_to_your_drive/test_out",
   "ADNI_PROCESSED": "/path_to_your_drive/data.tsv",
   "ADNI_VERSION": 3
}
```

Step 5

1. Initialize ExploreASL
2. Run xASL_adni_Convert2Source
3. Run xASL_adni_Convert2BIDS

Step 6

Give path to dataPar file, which will be generated automatically after conversion

Example Shown below:

dataPar=

'/path_to_your_drive/test_out/014_S_4039/derivatives/ExploreASL/dataPar.json';

[x] = ExploreASL_Master (dataPar,0,1)

Step 7

For specific regions add Atlas in the dataPar.json file

5.2.8 Statistical Analysis

Differences between AD and Controls

We found the differences between AD and Controls for the variables cholic acid and MMSE score, using statistical testing. Likewise, we arrived at the differences between AD and Controls for the variables CBF and amyloid-SUVR regarding (i) whole brain (ii) precuneus (ii) hippocampus (iii) cingulate. We tested the distributions of each variable for normality (using Anderson-Darling test). Thereby, we found CBF and SUVR- amyloid to be normal distributions; hence the student unpaired t-test was used (Fig.S2.1). On other hand, we found that MMSE and cholic acid were not normal distributions (Fig.S2.2), hence nonparametric assessment (Kolmogorov-Smirnov test) was utilized. We find that the differences between AD and controls are highly significant for all our variables: - Cholic acid: $p = 0.0487$; CBF: $p < 0.0001$; SUVR-amyloid: $p < 0.0001$; and MMSE: $p < 0.001$.

A)

Test for normal distribution	CN-CBF	AD-CBF
Anderson-Darling test		
A2*	0.2936	0.5508
P value	0.5876	0.1483
Passed normality test (alpha=0.05)?	Yes	Yes
P value summary	ns	ns
D'Agostino & Pearson test		
K2	1.326	1.975
P value	0.5152	0.3726
Passed normality test (alpha=0.05)?	Yes	Yes
P value summary	ns	ns
Shapiro-Wilk test		
W	0.975	0.9657
P value	0.3634	0.1545
Passed normality test (alpha=0.05)?	Yes	Yes
P value summary	ns	ns
Kolmogorov-Smirnov test		
KS distance	0.0691	0.1193
P value	>0.1000	0.0727
Passed normality test (alpha=0.05)?	Yes	Yes
P value summary	ns	ns
Number of values	50	50

B)

Test for normal distribution	CN-SUVR	AD-SUVR
Anderson-Darling test		
A2*	0.5372	0.4885
P value	0.1607	0.2131
Passed normality test (alpha=0.05)?	Yes	Yes
P value summary	ns	ns
D'Agostino & Pearson test		
K2	2.386	2.021
P value	0.3033	0.3641
Passed normality test (alpha=0.05)?	Yes	Yes
P value summary	ns	ns
Shapiro-Wilk test		
W	0.9756	0.965
P value	0.386	0.1441
Passed normality test (alpha=0.05)?	Yes	Yes
P value summary	ns	ns
Kolmogorov-Smirnov test		
KS distance	0.09888	0.1028
P value	>0.1000	>0.1000
Passed normality test (alpha=0.05)?	Yes	Yes
P value summary	ns	ns
Number of values	50	50

Figure S2.1 Normality test for (A) CBF and (B) SUVR-amyloid.

A)

	CN-Cholic Acid	AD-Cholic Acid
Test for normal distribution		
Anderson-Darling test		
A2*	35.04	21.58
P value	<0.0001	<0.0001
Passed normality test (alpha=0.05)?	No	No
P value summary	****	****
D'Agostino & Pearson test		
K2	192.9	124.1
P value	<0.0001	<0.0001
Passed normality test (alpha=0.05)?	No	No
P value summary	****	****
Shapiro-Wilk test		
W	0.447	0.5484
P value	<0.0001	<0.0001
Passed normality test (alpha=0.05)?	No	No
P value summary	****	****
Kolmogorov-Smirnov test		
KS distance	0.3335	0.3073
P value	<0.0001	<0.0001
Passed normality test (alpha=0.05)?	No	No
P value summary	****	****
Number of values	182	136

B)

	MMSE-CN	MMSE-AD
Test for normal distribution		
Anderson-Darling test		
A2*	4.035	1.061
P value	<0.0001	0.0079
Passed normality test (alpha=0.05)?	No	No
P value summary	****	**
D'Agostino & Pearson test		
K2	6.948	11.07
P value	0.031	0.004
Passed normality test (alpha=0.05)?	No	No
P value summary	*	**
Shapiro-Wilk test		
W	0.794	0.9191
P value	<0.0001	0.0022
Passed normality test (alpha=0.05)?	No	No
P value summary	****	**
Kolmogorov-Smirnov test		
KS distance	0.272	0.1328
P value	<0.0001	0.0276
Passed normality test (alpha=0.05)?	No	No
P value summary	****	*
Number of values	50	50

Figure S2.2 Normality test for (A) Cholic acid, and (B) MMSE.

Sample size calculation

We have made the sample size calculation, which shows that for proper statistical power (α= 0.05%, β = 0.2, and power = 80%), the sample size needed for serum cholic acid is 26 (Fig. S3.A). Similarly, we calculated the sample size for ASL – CBF (Fig. S3.B), to be 9. Likewise, we found sample size of PET-AV45 (amyloid) as 17 (Fig. S3.C).

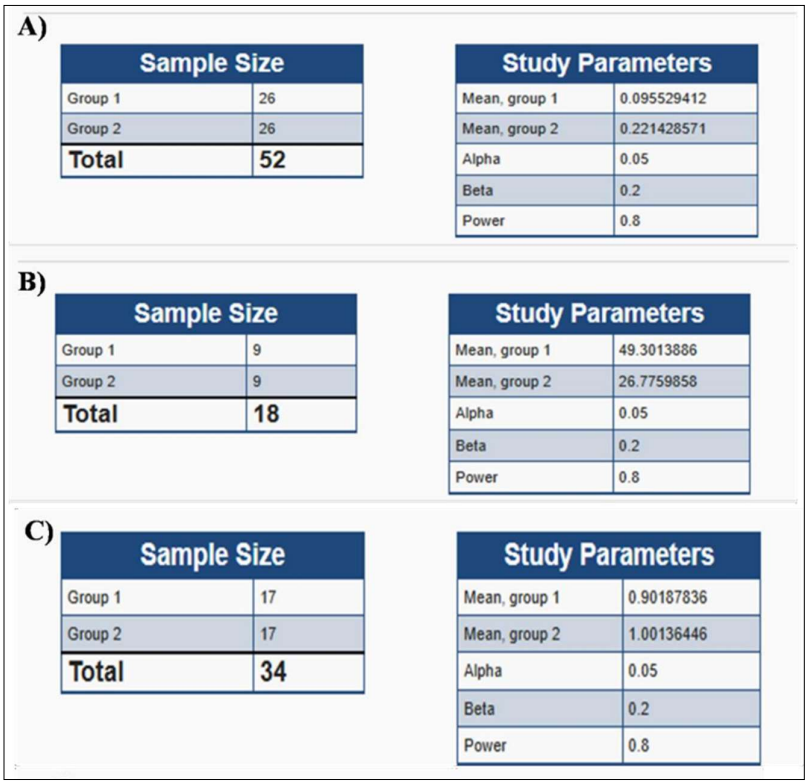

Figure S3. Power analysis for calculation of minimum sample size required with power of 80%: (A) Serum cholic acid, (B) Cerebral blood flow - ASL, and (C) PET-AV45 amyloid level.

5.3.7 Cholic acid causatively influences Amyloid-β load

https://www.real-statistics.com/time-series-analysis/time-series-miscellaneous/granger-causality/

Granger Causality

As we have learnt on several times, correlation does not always indicate causation, and although we may quantify the degree of link between two variables, i.e. correlation, determining whether one variable causes another one is more difficult.

Although we do not think that a current or future event may cause a previous event in general, we do believe that a past event can trigger a present or future occurrence. This serves as the impetus for the Granger's Causality test on time-series data, which provides proof that variable x causes variable y.

Observation: The Granger Causality test is based on the assumption that both the x and y time series are stationary. If this is not the case, then prior to conducting the Granger Causality test, differencing, de-trending, or other procedures must be used.

Age	Cholic Acid	SUVR	CBF
59	0.036	0.888853	26.36605
60	0.017	1.073577	20.43635
61	0.028	0.953749	23.18505
62	0.049	0.981735	20.68335
63	0.052	0.917114	25.16875
64	0.045	1.050734	21.18602
65	0.024	1.033675	18.66852
66	0.048	1.235607	22.13161
67	0.014	1.00795	26.35295
68	0.013	0.90258	26.73195
69	0.02	0.948123	25.6973
70	0.035	1.279058	20.18714
71	0.022	0.963619	27.9429
72	0.16	0.817118	34.6204
73	0.018	1.052991	28.6909
74	0.01	0.96754	24.49475
75	0.186	0.955653	38.69985

Figure 1: Serum cholic acid level, amyloid load and cerebral blood flow.

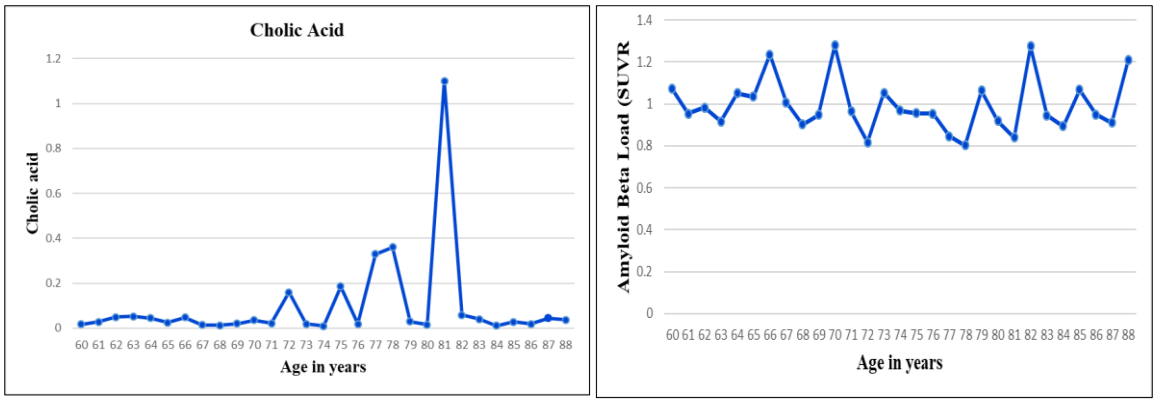

Figure 2: Time series plots

As a result, we will instead study the first differences of each time series. The data and time series plots for these are shown in Figure 3.

Age	Cholic Aci	SUVR
59		
60	-0.019	0.184724
61	0.011	-0.11983
62	0.021	0.027986
63	0.003	-0.06462
64	-0.007	0.13362
65	-0.021	-0.01706
66	0.024	0.201932
67	-0.034	-0.22766
68	-0.001	-0.10537
69	0.007	0.045543
70	0.015	0.330935
71	-0.013	-0.31544
72	0.138	-0.1465
73	-0.142	0.235873
74	-0.008	-0.08545
75	0.176	-0.01189

Figure 3: Differenced time series

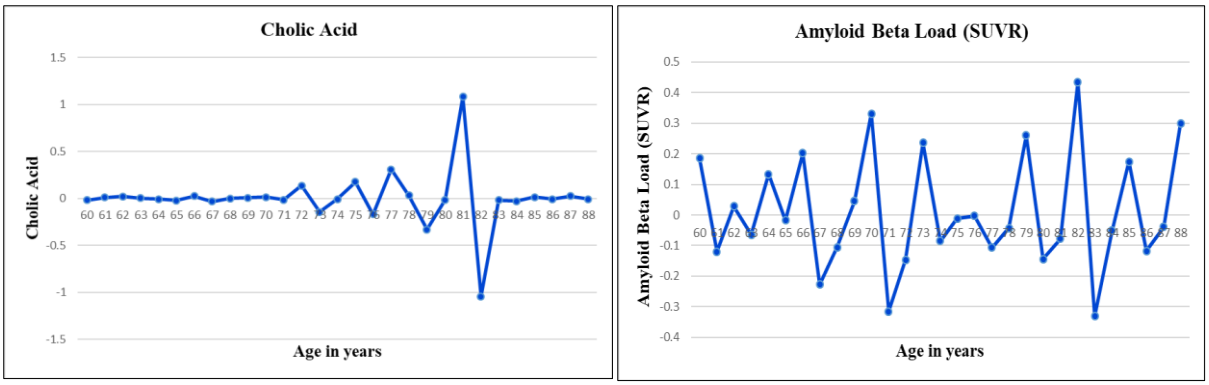

Figure 4: Plots for differenced time series

The plots suggest that the time series may be stationary. This result is confirmed by using the ADF test [Augmented Dickey-Fuller Test | Real Statistics Using Excel (real-statistics.com)].

ADF Test	CA
criteria	schwert
drift	no
trend	no
lag	9
alpha	0.05
tau-stat	-4.50194
tau-crit	-1.95254
stationary	yes
aic	-0.05929
bic	-0.01214
lags	0
coeff	-0.83982
p-value	< .01

ADF Test	SUVR
criteria	schwert
drift	no
trend	no
lag	9
alpha	0.05
tau-stat	-8.69155
tau-crit	-1.95298
stationary	yes
aic	-1.03828
bic	-0.94229
lags	1
coeff	-2.35834
p-value	< .01

Figure 5: ADF tests

We now show how to determine whether Cholic Acid Granger-cause Amyloid load for lags = 5. To do this we perform regression on the X data in range E2:N26 of Figure 6 and Y data in range O2:O26.

E	F	G	H	I	J	K	L	M	N	O
CA1	CA2	CA3	CA4	CA5	AB1	AB2	AB3	AB4	AB5	AB
-0.007	0.003	0.021	0.011	-0.019	0.13362	-0.06462	0.027986	-0.11983	0.184724	-0.01706
-0.021	-0.007	0.003	0.021	0.011	-0.01706	0.13362	-0.06462	0.027986	-0.11983	0.201932
0.024	-0.021	-0.007	0.003	0.021	0.201932	-0.01706	0.13362	-0.06462	0.027986	-0.22766
-0.034	0.024	-0.021	-0.007	0.003	-0.22766	0.201932	-0.01706	0.13362	-0.06462	-0.10537
-0.001	-0.034	0.024	-0.021	-0.007	-0.10537	-0.22766	0.201932	-0.01706	0.13362	0.045543
0.007	-0.001	-0.034	0.024	-0.021	0.045543	-0.10537	-0.22766	0.201932	-0.01706	0.330935
0.015	0.007	-0.001	-0.034	0.024	0.330935	0.045543	-0.10537	-0.22766	0.201932	-0.31544
-0.013	0.015	0.007	-0.001	-0.034	-0.31544	0.330935	0.045543	-0.10537	-0.22766	-0.1465
0.138	-0.013	0.015	0.007	-0.001	-0.1465	-0.31544	0.330935	0.045543	-0.10537	0.235873
-0.142	0.138	-0.013	0.015	0.007	0.235873	-0.1465	-0.31544	0.330935	0.045543	-0.08545

Figure 6: Setup for regression

Q	R	S	T	U	V	W
Regression Analysis						
OVERALL FIT						
Multiple R	0.851381		AIC	-86.6504		
R Square	0.724849		AICc	-58.2867		
Adjusted R Squar	0.513194		SBC	-73.6918		
Standard Error	0.141282					
Observations	24					
ANOVA				Alpha	0.05	
	df	*SS*	*MS*	*F*	*p-value*	*sig*
Regression	10	0.683587	0.068359	3.424677	0.020508	yes
Residual	13	0.259488	0.019961			
Total	23	0.943075				

Figure 7: Test for Granger Causality

Since p-value = 0.020508 is small, we conclude that Cholic Acid Granger-cause Amyloid Load for lags = 5. Alternatively, we could have calculated the p-value by placing the Real Statistics formula =RSquareTest (E3:N26, E3:I26, O3:O26) in cell V13.

Real Statistics Functions: The Real Statistics Resource Pack supports the following two functions that make it easy to determine whether the time series in the column array Rx

Granger-causes the time series in the column array Ry at the stated number of lags.

GRANGER (Rx, Ry, lags) = the F statistic of the test

GRANGER_TEST (Rx, Ry, lags) = p-value of the test

We can use the GRANGER_TEST function to determine whether Cholic Acid Granger-causes Amyloid Load and vice versa at various number of lags, as shown in Figure 8.

Amyloid load causatively alters Cholic acid			*Cholic acid causatively alters Amyloid load.*		
k = no. of lags	F-statistic	*p*-value	*k* = no. of lags	F-statistic	*p*-value
1	3.95	0.06	***1***	***7.63***	***0.01***
2	0.54	0.59	2	2.07	0.15
3	1.11	0.37	3	1.50	0.25
4	0.77	0.56	4	1.28	0.32
5	0.49	0.78	5	0.85	0.54

Figure 8: Granger Causality Tests

We see from Figure 8 that Cholic Acid Granger-causes Amyloid Load, but the reverse is not true.

7.3.4 Diffusivity parameters alteration in Alzheimer's Disease

Comparison between Alzheimer's patients and healthy control subjects

We performed tractography analysis on AD patients and normal subjects and the tensor metrics were estimated (axial, radial and mean diffusivities). The quantitative analyses are shown in the Tables S1-S3 below.

Table S1: Structural integrity measures of tracts in Segment-1 region (amenable to metformin).

Tracts between affected regions	Parameters	Abbreviation	Control Mean	Alzheimer's Mean	*p*	R^2	f^2
Orbitofrontal cortex-Uncinate region	Diffusivity Measurements	MD	0.85	0.97	**0.0003**	**0.82**	**$(2.16)^2$**
		AxD	1.24	1.38	**0.0039**	**0.67**	**$(1.42)^2$**
		RD	0.65	0.77	**0.0010**	**0.76**	**$(1.80)^2$**

Table S2: Structural integrity measures of tracts in Segment-2 region (amenable to cilostazol).

Tracts between affected regions	Parameters	Abbreviations	Control Mean	Alzheimer's Mean	*p*	R^2	f^2
Parietal Lobes-Inferior frontal region	Diffusivity Measurements	MD	0.79	0.85	**0.0015**	**0.73**	**$(2.76)^2$**
		AxD	1.19	1.27	**0.0028**	**0.69**	**$(2.26)^2$**
		RD	0.59	0.64	**0.0050**	**0.65**	**$(1.84)^2$**

Table S3: Structural integrity measures of tracts in Segment-3 region (amenable to rifampicin).

Tracts between affected regions	Parameters	Abbreviation	Control Mean	Alzheimer's Mean	*p*	R^2	f^2
Posterior Cingulate Cortex - Parietal Association Cortex	Diffusivity Measurements	MD	0.77	0.90	**0.0001**	**0.85**	**$(2.38)^2$**
		AxD	1.15	1.27	**0.0052**	**0.64**	**$(1.34)^2$**
		RD	0.58	0.71	**0.0001**	**0.88**	**$(2.72)^2$**

For all the segments and for all the diffusivity parameters, we see that the all the three diffusivities of Alzheimer's subjects exceed those of normal control subjects, and in all these cases, theincrease is highly significant ($p \leq 0.005$).

Sample size calculation:

Thereafter, for each segment-1,2 and 3, we performed a power analysis using the diffusivities (MD, AxD, RD) in the two groups (Alzheimer's patients and control subjects), using the power = 80%, α = 0.05% and β = 0.020. For instance, regarding segment-2, we first considered the MD diffusivity (Table S2, upper row), where the mean values of MD are given for the two groups. Thereby, we calculated the sample size as shown below (Figure S2). As one can see, the sample size required is 4. We implemented such sample size calculation for every segment for each diffusivity and found that the sample size is 4 or 5. We note the sample size of our present study is n_1=n_2=5 satisfies the minimum sample size calculated, hence our pilot investigation in this report can be taken as satisfactory.

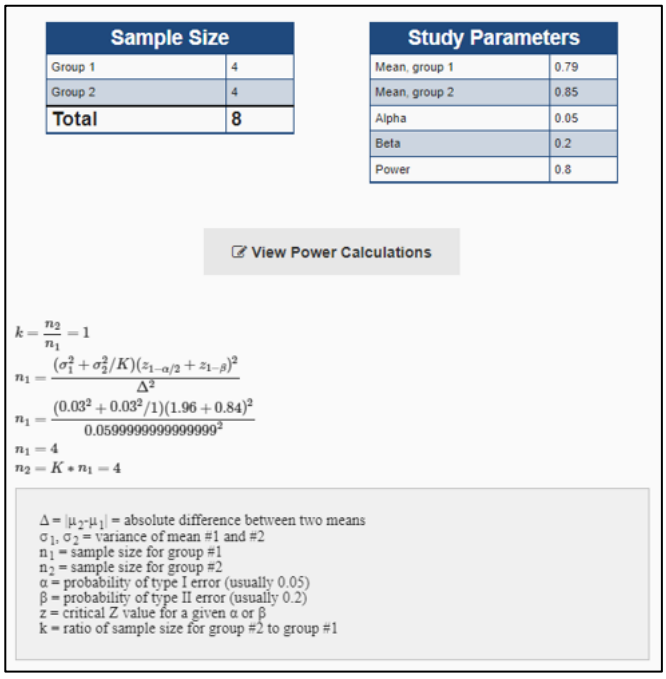

Figure S2. Power analysis for calculation of minimum sample size required with power of 80%.

Analysis of Effect-size

Subsequently we investigated the intensity of the effect size due to the increase of the diffusivities in Alzheimer's patient with respect to control subjects. For this, Cohen's formulation was used for the effect size. As per this formulation, $\eta^2 = R^2$, whence $f^2=[\eta/(1-\eta)]$. Thereby, we calculated the effect size f^2 for all the diffusivity parameters in all the anatomical segments (Tables S1, S2, S3). It is known that if $f^2 > (0.4)^2$, then there is large effect size. Since the values of f^2 in those Tables are well above this threshold of $(0.4)^2$, it can be indicated that the increase of diffusivity, i.e., loss of fibre integrity, has large effect size.

7.3.6 Identification of expression of the genes

Gene Analysis

L	M	N	O	P	Q	R
structure_abbreviation	structure_color	top_level_structure_id	top_level_structure_name	top_level_structure_abbreviation	top_level_structure_color	1049479-ABCB1
SC	98653	9001	mesencephalon	MES	0E7911	-1.8183
Hb	85E872	4520	epithalamus	ET	7AE872	-1.7625
PTec	99033	9001	mesencephalon	MES	0E7911	-1.6472
LOrG	E8CA59	4009	frontal lobe	FL	E8CD59	-1.638
CPLV	872601	9352	sulci & spaces	SS	6D6E70	-1.638

Figure S3: Ranked expression levels of gene ABCB1 downregulated in various brain structures. The relevant region is underlined.

F	G	H	I	J	K	L	M	N	O	P	Q	R
sample_p	sample_n	sample_n	sample_n	structure_	structure_	structure_	structure_	top_level_	top_level_structure_	top_level_	top_level_	105949-
1.13E+08	126	116	117	12893	CA2 field	CA2	FFBF66	4249	hippocampal format	HiF	FFC466	-2.6536
1.2E+08	102	160	127	9528	cochlear n	8Co	0A52B7	9512	myelencephalon	MY	1F67CC	-2.5452
1.59E+08	99	122	85	12913	arcuate nu	ARH	7FFF97	4540	hypothalamus	Hy	7FFF90	-2.2626
1.46E+08	94	138	138	4713	X	Ve-X	00D5E8	4697	cerebellar cortex	CbCx	00D5E8	-2.1036
1.12E+08	114	105	129	12891	dentate gy	DG	FFB566	4249	hippocampal format	HiF	FFC466	-2.0231

Figure S4: Ranked expression levels of gene ABCA1 downregulated in various brain structures. The relevant region is underlined.

9.3.4.1 Targets Prediction Results

Table S4: Gene ontology analysis of Ceftriaxone		
Gene Ontology	**Category**	**Genes Involved**
Molecular Function	binding (GO:0005488)	TNF, IL10RA, CXCL8, IL6ST
	molecular function regulator (GO:0098772)	TNF, CXCL8
	molecular transducer activity (GO:0060089)	IL10RA, IL6ST
Biological Process	biological regulation (GO:0065007)	TNF, IL10RA, IL1R1, CXCL8, IL6ST, IL1B
	cellular process (GO:0009987)	TNF, IL10RA, CXCL8, IL6ST, IL1B
	immune system process (GO:0002376)	CXCL8
	interspecies interaction between organisms (GO:0044419)	CXCL8, IL1B
	localization (GO:0051179)	CXCL8
	locomotion (GO:0040011)	CXCL8
	metabolic process (GO:0008152)	TNF, IL1B
	response to stimulus (GO:0050896)	TNF, IL10RA, IL1R1, CXCL8, IL6ST, IL1B
	signaling (GO:0023052)	TNF, IL10RA, CXCL8, IL6ST, IL1B
Cellular Component	cellular anatomical entity (GO:0110165)	TNF, IL10RA, CXCL8, IL6ST, IL1B
	protein-containing complex (GO:0032991)	IL6ST
Protein Class	defense/immunity protein (PC00090)	HLA-DRA
	intercellular signal molecule (PC00207)	IFNG, CXCL8, IL1B
	transmembrane signal receptor (PC00197)	IL10RA, IL1R1, IL6ST
Pathway	Apoptosis signaling pathway (P00006)	TNF
	CCKR signaling map (P06959)	CXCL8
	Inflammation mediated by chemokine and cytokine signaling pathway (P00031)	IFNG, CXCL8, IL6, IL1B
	Interferon-gamma signaling pathway (P00035)	IFNG
	Interleukin signaling pathway (P00036)	IL10RA, CXCL8, IL6ST, IL6
	T cell activation (P00053)	HLA-DRA
	Wnt signaling pathway (P00057)	TNF
	p38 MAPK pathway (P05918)	IL1R1

Table S5: Gene ontology analysis of Minocycline		
Gene Ontology	**Category**	**Genes Involved**
Molecular Function	binding (GO:0005488)	CXCL10, STAT1, CCL2, CXCL8, CCL4, CCL5, CXCL9, CCL18
	molecular function regulator (GO:0098772)	CXCL10, STAT1, CCL2, CXCL8, CCL4, CCL5, CXCL9, CCL18
Biological Process	biological regulation (GO:0065007)	CXCL10, STAT1, CCL2, CXCL8, CCL4, CCL5, CXCL9, CCL18
	cellular process (GO:0009987)	CXCL10, STAT1, CCL2, CXCL8, CCL4, CCL5, CXCL9, CCL18
	immune system process (GO:0002376)	CXCL10, STAT1, CCL2, CXCL8, CCL4, CCL5, CXCL9, CCL18
	interspecies interaction between organisms (GO:0044419)	CXCL10, STAT1, CCL2, CXCL8, CCL4, CCL5, CXCL9, CCL18
	localization (GO:0051179)	CXCL10, CCL2, CXCL8, CCL4, CCL5, CXCL9, CCL18
	locomotion (GO:0040011)	CXCL10, CCL2, CXCL8, CCL4, CCL5, CXCL9, CCL18
	metabolic process (GO:0008152)	STAT1, CCL2, CCL4, CCL5, CCL18
	response to stimulus (GO:0050896)	CXCL10, STAT1,CCR5, CCL2, CXCL8, CCL4, CCL5, CXCL9, CCL18
	signaling (GO:0023052)	CXCL10, STAT1, CCL2, CXCL8, CCL4, CCL5, CXCL9, CCL18
Cellular Component	cellular anatomical entity (GO:0110165)	CXCL10, STAT1,CCR5, CCL2, CXCL8, CCL4, CCL5, CXCL9, CCL18
	intracellular (GO:0005622)	STAT1, CCR5
Protein Class	gene-specific transcriptional regulator (PC00264)	STAT1
	intercellular signal molecule (PC00207)	CXCL10, CCL2, IFNG, CXCL8, CCL4, CCL5, CXCL9, CCL18
Pathway	Angiogenesis (P00005))	STAT1
	CCKR signaling map (P06959)	CXCL8
	EGF receptor signaling pathway (P00018)	STAT1
	Inflammation mediated by chemokine and cytokine signaling pathway (P00031)	CXCL10, STAT1,CCR5, CCL2, IFNG, CXCL8, CCL4, CCL5, CXCL9, CCL18
	Interferon-gamma signaling pathway (P00035)	STAT1, IFNG
	Interleukin signaling pathway (P00036)	STAT1, CXCL8
	JAK/STAT signaling pathway (P00038)	STAT1

Table S6: Gene ontology analysis of Podophyllotoxin		
Gene Ontology	**Category**	**Genes Involved**
Molecular Function	binding (GO:0005488)	STAT1, ITGB2, IRF2, IRF3, JUN, IRF9, ICAM1, STAT3, IRF1
	molecular function regulator (GO:0098772)	STAT1, IRF2, IRF3, JUN, IRF9, STAT3, IRF1
Biological Process	biological adhesion (GO:0022610)	ITGB2, ICAM1
	biological regulation (GO:0065007)	STAT1, ITGB2, IRF2, IRF3, JUN, IRF9, STAT3, IRF1
	cellular process (GO:0009987)	STAT1, ITGB2, IRF2, IRF3, JUN, IRF9, ICAM1, STAT3, IRF1
	immune system process (GO:0002376)	STAT1
	interspecies interaction between organisms (GO:0044419)	STAT1
	localization (GO:0051179)	ITGB2
	locomotion (GO:0040011)	ITGB2
	metabolic process (GO:0008152)	STAT1, IRF2, IRF3, JUN, IRF9, STAT3, IRF1
	response to stimulus (GO:0050896)	STAT1, ITGB2, STAT3
	signaling (GO:0023052)	STAT1, ITGB2, STAT4
Cellular Component	cellular anatomical entity (GO:0110165)	STAT1, ITGB2, IRF2, IRF3, JUN, IRF9, ICAM1, STAT3, IRF1
	intracellular (GO:0005622)	STAT1, IRF2, IRF3, JUN, IRF9, STAT3, IRF1
	protein-containing complex (GO:0032991)	ITGB2, JUN
Protein Class	cell adhesion molecule (PC00069)	ITGB2
	gene-specific transcriptional regulator (PC00264)	STAT1, IRF2, IRF3, JUN, IRF9, STAT3, IRF1
	intercellular signal molecule (PC00207)	IFNG
Pathway	Angiogenesis (P00005))	STAT1, JUN, STAT3
	CCKR signaling map (P06959)	JUN, STAT3
	EGF receptor signaling pathway (P00018)	STAT1, STAT3
	Inflammation mediated by chemokine and cytokine signaling pathway (P00031)	STAT1, ITGB2, IFNG, JUN, STAT3
	Interferon-gamma signaling pathway (P00035)	STAT1, IFNG
	Interleukin signaling pathway (P00036)	STAT1, STAT3
	JAK/STAT signaling pathway (P00038)	STAT1, STAT3

Table S7: Gene ontology analysis of Chlorogenic Acid		
Gene Ontology	**Category**	**Genes Involved**
Molecular Function	binding (GO:0005488)	MAFG, NOS3, JUN, HIF1A, NFE2, NFE2L2, MAFK, ATP2B1
	catalytic activity (GO:0003824)	MTOR, NOS3, ATP2B1
	molecular function regulator (GO:0098772)	MAFG, JUN, HIF1A, NFE2, NFE2L2, MAFK
	transporter activity (GO:0005215)	ATP2B1
Biological Process	biological regulation (GO:0065007)	MAFG, NOS3, MTOR, JUN, HIF1A, NFE2, NFE2L2, MAFK, ATP2B1
	cellular process (GO:0009987)	MAFG, NOS3, MTOR, JUN, HIF1A, NFE2, NFE2L2, MAFK, ATP2B1, IL1B
	developmental process (GO:0032502)	MAFG, NOS3
	interspecies interaction between organisms (GO:0044419)	NOS3, IL1B
	metabolic process (GO:0008152)	MAFG, NOS3, MTOR, JUN, HIF1A, NFE2, NFE2L2, MAFK, IL1B
	multi-organism process (GO:0051704)	NOS3
	multicellular organismal process (GO:0032501)	MAFG, NOS3
	reproduction (GO:0000003)	NOS3
	reproductive process (GO:0022414)	NOS3
	response to stimulus (GO:0050896)	MTOR, NOS3, HIF1A, NFE2L2, IL1B
	signaling (GO:0023052)	MTOR, NOS3, IL1B
Cellular Component	cellular anatomical entity (GO:0110165)	MAFG, NOS3, MTOR, JUN, HIF1A, NFE2, NFE2L2, MAFK, ATP2B1, IL1B
	intracellular (GO:0005622)	MAFG, NOS3, MTOR, JUN, HIF1A, NFE2, NFE2L2, MAFK, ATP2B1, IL1B
	protein-containing complex (GO:0032991)	MTOR, JUN
Protein Class	gene-specific transcriptional regulator (PC00264)	MAFG, JUN, HIF1A, NFE2, NFE2L2, MAFK
	intercellular signal molecule (PC00207)	IL1B
	metabolite interconversion enzyme (PC00262)	NOS3
	nucleic acid metabolism protein (PC00171)	NOS3
	protein modifying enzyme (PC00260)	MTOR
	transporter (PC00227)	ATP2B1
	Angiogenesis (P00005)	JUN, NOS3, HIF1A
	Apoptosis signaling pathway (P00006)	JUN
	B cell activation (P00010)	JUN

Pathway	CCKR signaling map (P06959)	JUN
	Hypoxia response via HIF activation (P00030)	MTOR, HIF1A
	Inflammation mediated by chemokine and cytokine signaling pathway (P00031)	JUN, IL1B
	Interleukin signaling pathway (P00036)	MTOR, NOS3
	PDGF signaling pathway (P00047)	MTOR, JUN
	T cell activation (P00053)	JUN
	Toll receptor signaling pathway (P00054)	JUN
	VEGF signaling pathway (P00056)	NOS3, HIF1A

Table S8: Gene ontology analysis of Naringenin		
Gene Ontology	**Category**	**Genes Involved**
Molecular Function	binding (GO:0005488)	STAT1, FAS, TNFRSF1A, JUN, TP53, STAT3, CREBBP
	catalytic activity (GO:0003824)	AKT1, CREBBP
	molecular function regulator (GO:0098772)	STAT1, JUN, TP53, STAT3, CREBBP
	molecular transducer activity (GO:0060089)	FAS, TNFRSF1A
Biological Process	biological regulation (GO:0065007)	STAT1, FASLG, FAS, JUN, TP53, AKT1, STAT3, CREBBP
	cellular process (GO:0009987)	STAT1, FASLG, FAS, JUN, TP53, AKT1, STAT3, CREBBP
	immune system process (GO:0002376)	STAT1 FAS
	interspecies interaction between organisms (GO:0044419)	STAT1
	metabolic process (GO:0008152)	STAT1, FASLG, FAS, TNFRSF1A, AKT1, STAT3
	response to stimulus (GO:0050896)	STAT1, FASLG, FAS, TNFRSF1A, AKT1, STAT3
	signaling (GO:0023052)	STAT1, FASLG, FAS, AKT1, STAT3
Cellular Component	cellular anatomical entity (GO:0110165)	STAT1, FAS, TNFRSF1A, JUN, TP53, STAT3, CREBBP
	intracellular (GO:0005622)	STAT1, TNFRSF1A, JUN, TP53, STAT3, CREBBP
	protein-containing complex (GO:0032991)	FAS, TNFRSF1A, JUN, CREBBP
Protein Class	chromatin/chromatin-binding, or -regulatory protein (PC00077)	CREBBP
	gene-specific transcriptional regulator (PC00264)	STAT1, JUN, TP53, STAT3
	protein modifying enzyme (PC00260)	AKT1
	transmembrane signal receptor (PC00197)	FAS, TNFRSF1A
Pathway	Angiogenesis (P00005)	STAT1, JUN, AKT1, STAT3
	Apoptosis signaling pathway (P00006)	FASLG, FAS, TNFRSF1A, JUN, TP53, AKT1, FADD
	B cell activation (P00010)	JUN
	CCKR signaling map (P06959)	JUN, AKT1, STAT3
	EGF receptor signaling pathway (P00018)	STAT1, AKT1, STAT3
	FAS signaling pathway (P00020)	FASLG, FAS, JUN, AKT1, FADD
	Hypoxia response via HIF activation (P00030)	AKT1, CREBBP
	Inflammation mediated by chemokine and cytokine signaling pathway (P00031)	STAT1, JUN, AKT1, STAT3
	Interleukin signaling pathway (P00036)	STAT1, AKT1, STAT3

	JAK/STAT signaling pathway (P00038)	STAT1, STAT3
	PDGF signaling pathway (P00047)	STAT1, JUN, STAT3
	T cell activation (P00053)	JUN, AKT1
	Toll receptor signaling pathway (P00054)	JUN
	VEGF signaling pathway (P00056)	AKT1

Table S9: Gene ontology analysis of Quercetin		
Gene Ontology	**Category**	**Genes Involved**
Molecular Function	binding (GO:0005488)	STAT1, CCL2, CXCL8, JUN, CCL5, CXCL1, STAT3, IRF1
	molecular function regulator (GO:0098772)	STAT1, CCL2, CXCL8, JUN, CCL5, CXCL1, STAT3, IRF1
Biological Process	biological regulation (GO:0065007)	STAT1, CCL2, CXCL8, JUN, CCL5, CXCL1, STAT3, IRF1
	cellular process (GO:0009987)	STAT1, CCL2, CXCL8, JUN, CCL5, CXCL1, STAT3, IRF1
	immune system process (GO:0002376)	STAT1, CCL2, CXCL8, CCL5, CXCL1
	interspecies interaction between organisms (GO:0044419)	STAT1, CCL2, CXCL8, CCL5, CXCL1
	localization (GO:0051179)	CCL2, CXCL8, CCL5, CXCL1
	locomotion (GO:0040011)	CCL2, CXCL8, CCL5, CXCL1
	metabolic process (GO:0008152)	STAT1, CCL2, JUN, CCL5, STAT3
	response to stimulus (GO:0050896)	STAT1, CCL2, CXCL8, JUN, CCL5, CXCL1, STAT3
	signaling (GO:0023052)	STAT1, CCL2, CXCL8, CCL5, CXCL1, STAT3
Cellular Component	cellular anatomical entity (GO:0110165)	STAT1, CCL2, CXCL8, JUN, CCL5, CXCL1, STAT3, IRF1
	intracellular (GO:0005622)	STAT1, JUN, STAT3, IRF1
	protein-containing complex (GO:0032991)	JUN
Protein Class	gene-specific transcriptional regulator (PC00264)	STAT1, JUN, STAT3, IRF1
	intercellular signal molecule (PC00207)	CCL2, IFNG, CXCL8, CCL5, CXCL1
Pathway	Angiogenesis (P00005))	STAT1, JUN, STAT3
	CCKR signaling map (P06959)	CXCL8, JUN, CXCL1, STAT3
	Inflammation mediated by chemokine and cytokine signaling pathway (P00031)	STAT1, CCL2, IFNG, CXCL8, JUN, CCL5, STAT3, IL6
	Interferon-gamma signaling pathway (P00035)	STAT1, IFNG
	Interleukin signaling pathway (P00036)	STAT1, CXCL8, STAT3, IL6
	PDGF signaling pathway (P00047)	STAT1, JUN, STAT3
	Ras Pathway (P04393)	STAT1, JUN, STAT3

List of publications

Peer reviewed papers

Bhattacharjee A, Purohit P, Roy PK, 2022. "Neuroprotective drug discovery from phytochemicals and metabolites for CNS infection: A systems biology approach with clinical and neuroimaging validation ", Frontiers in Neuroscience: Section Neuropharmacology, DOI: 10.3389/fnins.2022.917867.

Bhattacharjee A, Roy PK, 2022. "Conjoint hepatobiliary-enterohepatic cycles for amyloid excretion and enhancing its drug-induced clearance: a systems biology approach to Alzheimer's disease.", Journal of Biomolecular Structure and Dynamics, DOI: 10.1080/07391102.2022.2154842.

Bhattacharjee A, & Roy PK, 2023." MRI tractographic validation of drug-enhanced hepatic clearance of amyloid-beta and the therapeutic potential for Alzheimer's Disease: A Pilot Study.", Brain Disorders, DOI: 10.1016/j.dscb.2023.100112.

Bhattacharjee A, Roy PK, 2022. "Systems Analysis based approach for Therapeutic intervention in Mixed Vascular- Alzheimer Dementia (MVAD) using Secondary Metabolites", In book: Indopathy for Neuroprotection: Recent Advances, Bentham Science Publishers, DOI: 10.2174/9789815050868122010019.

Bhattacharjee A, Purohit P, Roy PK, 2023. "Neuroimaging-based drug discovery for amyloid clearance therapy in Alzheimer's disease using validated causation analysis", *(under review in Brain Connectivity).*

Ruttala R, Purohit P, **Bhattacharjee A,** Kumari B, Roy PK. 2022. "MRI-DTI Imaging Reveals Specific Neuro- degeneration Signature in Precuneus Node of Awareness Processing in Brain under Alzheimer's Disease", Journal of advanced applied scientific research. DOI:10.46947/joaasr442022460.

Kumari B, Sakode C, Lakshminarayan R, Purohit P, **Bhattacharjee A,** Roy PK, 2022. "A Mechanistic Analysis of Spontaneous Cancer Remission Phenomenon: Identification of Genomic Basis and Effector Biomolecules for Therapeutic Applicability", 3 Biotech, DOI:10.1007/s13205-023-03515-0.

Publications other than Ph.D. work

Bhattacharjee A, Prajapati SK, Krishnamurthy S, 2021. "Supplementation of taurine improves ionic homeostasis and mitochondrial function in the rats exhibiting post-traumatic stress disorder-like symptoms". European Journal of Pharmacology, DOI: 10.1016/j.ejphar.2021.174361.

Verma H, **Bhattacharjee A,** Shivavedi N, Nayak PK, 2022. "Evaluation of rosmarinic acid against myocardial infarction in maternally separated rats". Naunyn-Schmiedeberg's Archives of Pharmacology, DOI: 10.1007/s00210- 022-02273-9.

Verma H, **Bhattacharjee A,** Nayak PK, Roy PK, 2023 "Cardioprotective Effect of Rosmarinic Acid in Combined Stress Model of Wistar Rats validated with In-Silico and Experimental studies", (*under preparation*).

Conference abstracts

Bhattacharjee A, Roy PK, "A Systems Biology Methodology to Drug Discovery for Neurotropic Virus Infection with Clinical Corroboration" Proc. FENS-Forum, Paris, France, 09-13 July, 2022.

Bhattacharjee A, Roy PK, "An Integrated Systemic Approach to Amyloid Transportation and its Neuromodulation," Proc. IBRO-APRC, Punjab University, 04-09 November 2019.

Akshi, Kalra, Choudhary, Dipani A, **Bhattacharjee A,** Urai A, 2020. "Classifying fMRI data for context-dependent and context-independent language tasks", Bernstein Conference 2020, DOI: 10.12751/nncn. bc2020.0020.

Chowdhury S, Purohit P, **Bhattacharjee A,** Kumari B, Roy PK, "Novel Drug Discovery for Acute Encephalitis using A.I.-based machine-reading and knowledge-mapping of Medical Literature Text," Proc. 61st Annual Conference of National Academy of Medical Sciences, India, 26-28 Nov 2021

Baghel B, Kumari B, **Bhattacharjee A,** Purohit P, Roy PK, "Long-term Structural Stability observed in Cerebellum during Ageing: Radiological Genomics identifies Neuroprotective Drugs with Clinical Validation," Proc. 61st Annual Conference of National Academy of Medical Sciences, India, 26-28 Nov 2021